JOURNAL OF
biomaterials
applications

Soft Tissues and Materials

Journal of Biomaterials Applications
2019, Vol. 33(6) 792–807

DOI: 10.1177/0885328218811386
journals.sagepub.com/home/jba
SAGE

Freeze-dried chitosan-platelet-rich plasma implants improve supraspinatus tendon attachment in a transosseous rotator cuff repair model in the rabbit

Gabrielle Deprés-Tremblay[1], Anik Chevrier[1], Martyn Snow[2], Scott Rodeo[3] and Michael D Buschmann[4]

Abstract

Rotator cuff tears result in shoulder pain, stiffness, weakness and loss of motion. After surgical repair, high failure rates have been reported based on objective imaging and it is recognized that current surgical treatments need improvement. The aim of the study was to assess whether implants composed of freeze-dried chitosan (CS) solubilized in autologous platelet-rich plasma (PRP) can improve rotator cuff repair in a rabbit model. Complete tears were created bilaterally in the supraspinatus tendon of New Zealand White rabbits ($n = 4$ in a pilot feasibility study followed by $n = 13$ in a larger efficacy study), which were repaired using transosseous suturing. On the treated side, CS-PRP implants were injected into the transosseous tunnels and the tendon itself, and healing was assessed histologically at time points ranging from one day to two months post-surgery. CS-PRP implants were resident within transosseous tunnels and adhered to tendon surfaces at one day post-surgery and induced recruitment of polymorphonuclear cells from 1 to 14 days. CS-PRP implants improved attachment of the supraspinatus tendon to the humeral head through increased bone remodelling at the greater tuberosity and also inhibited heterotopic ossification of the supraspinatus tendon at two months. In addition, the implants did not induce any detectable deleterious effects. This preliminary study provides the first evidence that CS-PRP implants could be effective in improving rotator cuff tendon attachment in a small animal model.

Keywords

Rotator cuff, transosseous repair, chitosan, platelet-rich plasma, injectable implants, rabbit model

Introduction

Rotator cuff tears are one of the most common shoulder pathologies[1] and are associated with structural and architectural alterations of the musculotendinous unit, such as tendon retraction, muscular atrophy and fatty infiltration. Rotator cuff tears may cause chronic pain and severe functional disability, as well as compromise joint mechanics leading to degenerative joint changes. Rotator cuff tears often require surgical repair, and repair success is affected by numerous factors, including patients' age, number of tendons involved, and size of the tear.[2] Failure rates of up to 94%[3] have been reported, and tendon degeneration, hypovascularization, muscle atrophy, and lack of tendon-to-bone integration are some of the reasons proposed for failures.

The rotator cuff insertion site, also known as the enthesis, is never completely reformed after surgical reattachment.[4,5] Instead, healing occurs through synthesis of a fibrovascular disorganized scar tissue composed largely of type III collagen, which is biomechanically inferior, likely contributing to the

[1]Ecole Polytechnique de Montreal, Montreal, Canada
[2]The Royal Orthopaedic Hospital, Birmingham, UK
[3]The Hospital for Special Surgery, New York, NY, USA
[4]Ecole Polytechnique de Montreal, 2900 Boul Edouard-Montpetit, Montreal, Canada

Corresponding author:
Michael D Buschmann, Ecole Polytechnique de Montreal, 2900 Boul Edouard-Montpetit, Montreal H3T 1J4, QC Quebec, Canada.
Email: michael.buschmann@polymtl.ca

high rates of failure or incomplete healing. Patients with failed healing/re-tears can experience pain relief but usually continue to have compromised function. There have been attempts to improve rotator cuff repair with biological or synthetic tendon grafts or with augmentation techniques[6]; however, consistent healing of the rotator cuff following repair still remains an enormous clinical challenge.

Platelet-rich plasma (PRP) is a plasma fraction with a high platelet concentration that is obtained through centrifugation of whole blood.[7] Activation of platelets within PRP can be achieved by treatment with calcium chloride, thrombin, or contact with collagen, and leads to the release of several platelet-derived growth factors. The use of PRP to improve rotator cuff repair has been evaluated in both animal models and clinical studies since it is believed that growth factor release at the injury site could lead to cell proliferation, cell differentiation, and angiogenesis. However, the ability of PRP to improve rotator cuff repair is not supported by current clinical evidence.[8–11] Results have been inconsistent, possibly due to the lack of standardization of platelet separation techniques, variability in formulations of PRP used, as well as the short half-life, high diffusibility, and poor stability of PRP *in vivo*.

Chitosan (CS) is a biodegradable and biocompatible natural polymer obtained through chitin deacetylation.[12,13] In the context of cartilage repair, implants of CS-glycerol phosphate (GP)/blood have previously been shown by our research group to increase cell recruitment, vascularization and bone remodeling,[14,15] activate a beneficial phenotype of pro-wound healing macrophages,[16] and enhance tissue repair integration through osteoclast activity,[17] all of which are expected to be beneficial for rotator cuff repair. More recently, we have developed freeze-dried formulations of CS that can be solubilized in PRP to form injectable CS-PRP implants that coagulate *in situ*.[18] We have shown that chitosan inhibits platelet-mediated clot retraction and increases platelet-derived growth factor release from PRP *in vitro*.[19] The residency time and bioactivity of CS-PRP implants have also been shown *in vivo* to be superior to that of PRP alone.[18,19] Finally, CS-PRP implants were successfully used to augment cartilage and meniscus repair in small and large animal models.[20–22]

The aim of the current study was to assess whether CS-PRP implants can improve rotator cuff repair in a rabbit model. Surgical tears were created bilaterally in the supraspinatus (SSP) tendon of the rotator cuff of New Zealand White (NZW) rabbits, which were immediately repaired with transosseous suturing. On the treated side, CS-PRP implants were injected into the transosseous tunnels and the tendon itself. Healing was assessed histologically at time points ranging from one day to two months post-surgery. Our starting hypotheses were that: (1) CS-PRP implants would induce recruitment of polymorphonuclear cells (PMN) at early time points post-surgery, (2) CS-PRP implants would be degraded by two months post-surgery, and (3) CS-PRP implants would improve tendon healing through an increase in cell recruitment, angiogenesis, and bone remodeling.

Materials and methods

Rotator cuff tear model, surgical repair and study design

The protocol for this study was approved by the University of Montreal institutional committee (Protocol # 15–088, initial date of approval 3 September 2015) and was consistent with the Canadian Council on Animal Care guidelines for the care and use of laboratory animals. The bilateral rotator cuff tear model was first validated in a pilot feasibility study in four retired breeder female NZW rabbits aged 13 months (Table 1). Then, a larger efficacy study was performed using 13 skeletally mature female NZW rabbits aged 9 months (Table 2). The SSP tendon was exposed and a complete tear was created with a scalpel blade, as close as possible to the insertion site (Figure 1 (a)). The remaining stump was debrided, exposing the greater tuberosity. The tear was immediately repaired with a transosseous suturing technique described previously.[23–29] Briefly, an ~5 mm bony trough was drilled in the cancellous bone of the greater tuberosity using a high-speed microdrill (Ideal model, Geneq Scientific Instruments Inc) fitted with a 2.1 mm diameter drill bit (Fine Science Tools). Three 1.4 mm diameter drill holes were then drilled from the lateral aspect of the humerus to connect to the bony trough (Figure 1(b)).

Table 1. Design of study 1 – pilot feasibility study.

Group	Treatment shoulder 1	Treatment shoulder 2	# Animals/timepoints
1	Intact	Intact	$n = 1$ at day 0
2	Suturing + CS-PRP	Suturing + CS-PRP	$n = 1$ at day 1
3	Suturing + CS-PRP	Suturing	$n = 1$ at day 14 $n = 1$ at two months

Table 2. Design of study 2 – larger efficacy study.

Group	Treatment shoulder 1	Treatment shoulder 2	# Animals/time points
1	Intact	Intact	$n = 2$ at day 0
2	Suturing + CS-PRP[a]	Suturing + CS-PRP[1]	$n = 2$ at day 1
3	Suturing + CS-PRP	Suturing only	$n = 1$ at day 7
4	Suturing + CS-PRP	Suturing only	$n = 8$ at two months

[a]A Rhodamine-chitosan tracer was used in these animals for imaging purposes.

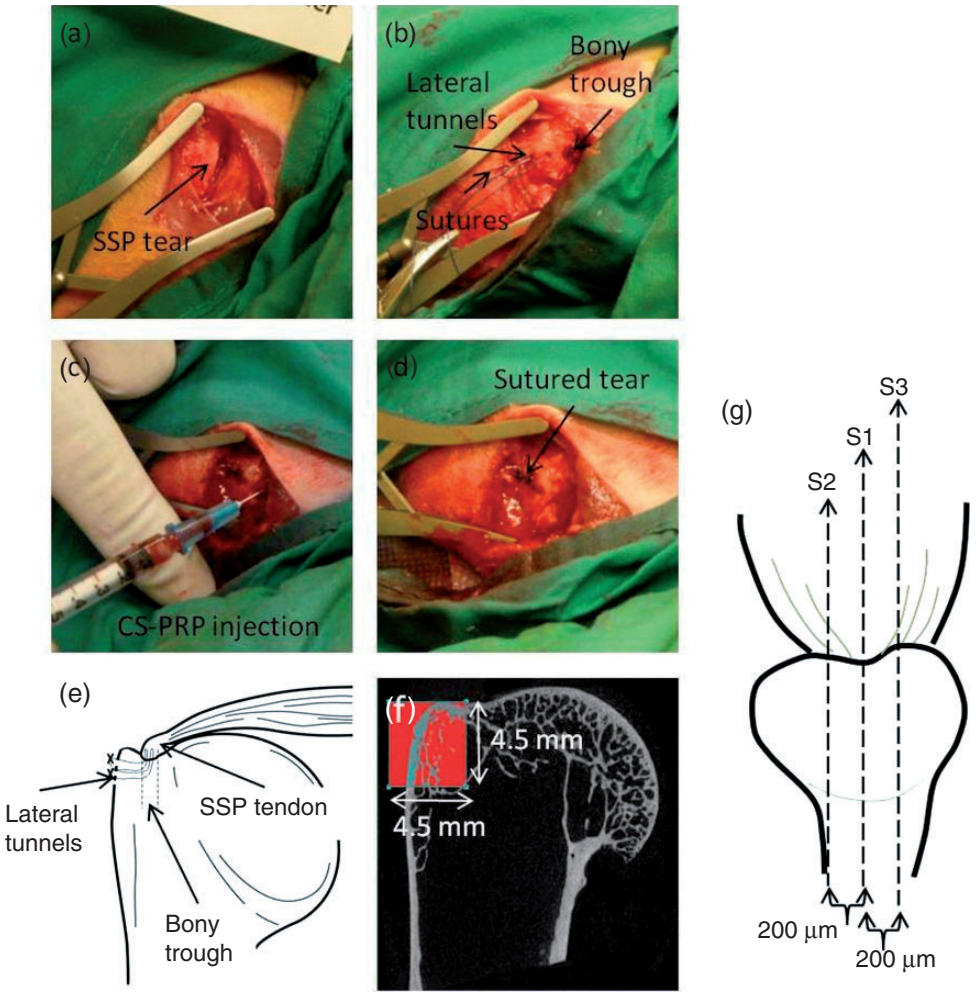

Figure 1. (a)–(d) Surgical procedure. A complete surgical tear was created in the supraspinatus (SSP) tendon of the rotator cuff, as close as possible to the insertion site (a). Two 3.0 prolene sutures were pre-placed through the bony trough, the lateral tunnels (b) and the tendon itself in a modified Mason-Allen pattern. In the case of treated shoulders, the CS-PRP mixture (150 µL) was injected into the bony trough prior to tightening the sutures (c), and it flowed out of all lateral tunnels. Sutures were tightened to attach the tendon to the humeral head (d). The CS-PRP mixture (150 µL) was then injected at the repaired insertion site and into the tendon itself. (e) Schematic representation of the surgical model. (f) Area in red is the region of interest (ROI) that was set over the greater tuberosity and used for micro-CT analysis. (g) Schematic representation of where histological sections were collected. Section 1 (S1) was collected roughly at the centre of the reattached SSP tendon. Section 2 (S2) and section 3 (S3) were systematically collected 200 µm away from section 1. All sections included the SSP tendon, attachment site and humeral head.

Cold irrigation with Ringer's lactate was used throughout drilling. Two 3.0 prolene sutures were passed through the lateral holes, the bony trough and the tendon itself in a modified Mason-Allen pattern. In treated shoulders, in addition to sutures, CS-PRP implants were applied as described below (Figure 1 (c)). Sutures were tightened over the lateral aspect of the humerus, thus pulling the tendon towards the

greater tuberosity (Figure 1(d)). The animals were allowed ad libitum cage activity postoperatively. Pain control was achieved with transdermal fentanyl patches for four days and two rabbits had rymadyl injections for three consecutive days for additional pain relief.

Preparation of freeze-dried chitosan formulations

Chitosan (raw material from Marinard) was deacetylated with sodium hydroxide (Sigma-Aldrich) and depolymerized with nitrous oxide (Sigma-Aldrich) in-house to produce a chitosan with 80.2% degree of deacetylation (DDA) and 36 kDa number average molar mass (M_n). This chitosan was used to prepare formulations containing 1% (w/v) chitosan, 28 mM HCl (Sigma-Aldrich), 1% (w/v) trehalose (Life Sciences) as a lyoprotecting agent and 42.2 mM $CaCl_2$ (Spectrum Chemicals) as a PRP activator.[18,19] This chitosan solution was filter-sterilized and 300 μL aliquots were distributed into sterile, de-pyrogenized 2cc glass vials and freeze-dried in three phases: (1) ramped freezing to −40°C in 1 h, isothermal 2 h at −40°C, (2) −40°C for 48 h, at 100 millitorrs, (3) ramped heating to 30°C in 12 h, isothermal 6 h at 30°C. Filter-sterile rhodamine-chitosan tracer[30] of corresponding M_n and DDA was added to eight of the vials for imaging purposes.

Preparation of PRP

Prior to surgery, 9 mL of blood was drawn from the rabbit ear artery and anti-coagulated with 1 mL 3.8% (w/v) sodium citrate (Sigma-Aldrich) (final citrate concentration 12.9 mM). The ACE EZ-PRP™ benchtop centrifuge was used to extract the PRP using a two-step centrifugation process.[31] Anti-coagulated blood was first centrifuged for 10 min at 1300 r/min. The supernatant and first 1–2 mm of erythrocyte fraction were removed and then centrifuged for 10 min at 2000 r/min. The bottom ~1.5 mL was retained and resuspended to make PRP. On average, the PRP contained 838 X 10E9/L platelets (4× the concentration in whole blood), 6.0 X 10E9/L leukocytes (1× the concentration in whole blood) and 1.7 X 10E12/L erythrocytes (0.3× the concentration in whole blood).

Solubilization of freeze-dried chitosan formulations in PRP and injection of CS-PRP implants

Freeze-dried chitosan formulations (300 μL was lyophilized in each vial) were solubilized with autologous PRP (300 μL) and injected using a 1-cc syringe equipped with a 25-gauge needle in two phases: (1) 150 μL injected prior to suturing the tendon, into the bony trough until it flowed out of the lateral tunnels and (2) 150 μL injected following suturing, within the SSP tendon itself and at the reattached insertion site. The rabbits were randomly divided into three groups (Tables 1 and 2): (1) Intact controls ($n = 3$ rabbits; 1 rabbit in Study 1 and 2 rabbits in Study 2); (2) animals treated bilaterally with suturing + CS-PRP and sacrificed at one day post-operative to assess implant distribution ($n = 3$ rabbits; 1 rabbit in Study 1 and 2 rabbits in Study 2); (3) animals treated with suturing + CS-PRP on one side and suturing only on the contralateral side and sacrificed at day 7 ($n = 1$ rabbit in Study 2), day 14 ($n = 1$ rabbit in Study 1) and at two months ($n = 9$ rabbits; one rabbit in Study 1 and eight rabbits in Study 2).

Specimen collection and histological processing

Both shoulders were dissected carefully to remove the SSP muscle, its tendon, and the proximal part of the humerus in one piece and the glenoid articular surface. SSP tendon attachment was scored macroscopically as intact/native (0), completely attached with tissue different from native (1), partially attached with tissue different from native (2) or detached (3). The SSP muscle-tendon–humeral head complex and the glenoid surfaces were fixed with 10% neutral buffered formalin (Fisher Scientific) and trimmed for further processing. The calcified tissues were decalcified with 0.5N HCl (Sigma-Aldrich) with trace glutaraldehyde (EMS). All samples were dehydrated in graded alcohol solutions and cleared in xylene (Fisher Scientific) for paraffin processing. Sections (5 μm thickness) were systematically collected at three sites (Figure 1(g)), stained with Iron hematoxylin/Safranin O/Fast Green (all from Sigma-Aldrich) and scanned with a Nanozoomer RS (Hamamatsu) for histological evaluation by two blinded observers (GDT and AC). Histological scoring of the SSP tendon (Table 3) and SSP tendon enthesis (Table 4) was based on systems reported previously.[32,33] Briefly, the SSP tendon was scored for cellularity, presence of tenocytes or inflammatory cells, vascularity, tissue organization, and heterotopic bone formation, with ranges between 0 (best score) and 3 (worst score). Inter-reader intraclass correlation coefficient (ICC) for the tendon scoring system was calculated with SAS Enterprise Guide 7.1 and SAS 9.4 (Toronto, ON, Canada) and was found to be excellent for five out of six categories (ICC > 0.90), and good for the heterotopic bone formation category (ICC = 0.68). The enthesis was scored for tendon attachment, attachment at anatomically correct location, presence of GAGs at the insertion site, and structural appearance of the enthesis, ranging between 0 (best score) and 2 (worst score) for the first three categories, and from 0 (best score) to 5 (worst score) for the last category. Inter-reader ICC was good for tendon attachment

Table 3. Microscopic scoring of SSP tendon.

Category to score		Score
I	Cellularity	
	Minimal	0
	Mild	1
	Moderate	2
	Marked	3
II	Tenocytes	
	Marked	0
	Moderate	1
	Mild	2
	Minimal	3
III	Inflammatory cells	
	None	0
	Mild	1
	Moderate	2
	Marked	3
IV	Vascularity	
	Minimal	0
	Mild	1
	Moderate	2
	Marked	3
V	Tissue organization	
	Native tendon	0
	Repair tissue mostly tendon-like	1
	Repair tissue a mixture of tendon-like tissue and highly cellular and vascular tissue	2
	Repair tissue highly cellular and vascular tissue	3
VI	Heterotopic bone formation within tendon, far from insertion site	
	None	0
	Mild	1
	Moderate	2
	Marked	3

Table 4. Microscopic scoring of SSP enthesis.

Category to score		Score
I	Tendon attachment	
	Complete	0
	Partial	1
	Gap	2
II	Attachment at anatomically normal site	
	Yes	0
	Partially	1
	No	2
III	Structural appearance of the enthesis	
	Native insertion with tidemark throughout	0
	Insertion has continuity with bone ingrowth and fibrocartilage and tidemark partially present	1
	Insertion has continuity with bone ingrowth and fibrocartilage cells but no tidemark	2
	Insertion has continuity with fibrous tissue	3
	Insertion has continuity with fat	4
	No continuity	5
IV	Glycosaminoglycans at insertion site	
	Normal	0
	Slight	1
	None	2

(ICC = 0.70) and excellent for attachment at anatomically correct location (ICC = 0.79), presence of GAGs at the insertion site (ICC = 0.80) and structural appearance of the enthesis (ICC = 0.95). Humeral head and glenoid articular surfaces were scored with the OARSI osteoarthritis cartilage histopathology assessment system.[34] Fatty infiltration in SSP muscle was scored as minimal (0), mild (1), moderate (2) or marked (3). A synovial fluid smear was collected by pipeting an aliquot of synovial fluid on a histological slide and stained with May-Grünwald-Giemsa for cell counting (percentage of leukocyte differential). Tissue harvesting, sectioning, staining, and analysis were all performed by the same personnel for both studies, within the same time frame.

Micro CT analysis

Prior to decalcification, the SSP tendon-humeral head complex was scanned using the Skyscan X-ray microtomography 1172 (Kontich, Belgium) with an aluminium filter at 14.1 μM pixel size resolutions and an X-ray source voltage of 56 kV, 1180 ms exposure, 0.45 rotation steps and three averaging frames. Images were reconstructed with NRecon software 1.6.1.5 (Kontich, Belgium), using the following parameters: smoothing of 2, ring artifact reduction of 10, beam-hardening correction of 40%. Datasets were repositioned with DataViewer software 1.4.3 (Kontich, Belgium). The region of interest (4.5 mm in the x-axis × 4.5 mm in the y-axis × 3 mm in the z-axis) was positioned on the edge of the greater tuberosity (Figure 1(f)) and 3D micro CT analysis was performed by using the global thresholding procedure in CTAn software 1.9.3.0 (Kontich, Belgium).

Statistical analysis

Scores from the two readers were averaged for each histological section. Statistical analyses were performed using SAS Enterprise Guide 7.1 and SAS 9.4 (Toronto, ON, Canada). The mixed model task was used to compare groups with post-hoc Tukey analysis to look at pairwise differences. The fixed effect was treatment (Intact vs. Sutures + CS-PRP vs. Sutures), the random effect was the rabbit number and the repeated effect was the section number. Data in the figures are presented as mean (circle); median (line); Box: 25th and 75th percentile; Whiskers: Box to the most extreme point within 1.5 interquartile range. $P < 0.05$ was considered statistically significant.

Results

CS-PRP implants adhered to SSP tendon tissue and were resident within the bony trough and lateral tunnels at one day post-surgery

At one day post-surgery, the attachment site of the SSP tendon was characterized by gap formation in all of the shoulders (Figure 2(a) and (e)). Despite our efforts, the stump of the SSP tendon was incompletely debrided in most cases (Figure 2(a) and (e)). The SSP tendons had areas that were structurally normal, and areas that had altered disorganized structure. Needle tracks containing CS-PRP implant were apparent in some cases (Figure 2(f)). In addition, CS-PRP implants were resident within the bony trough, the lateral tunnels and adhered to the tendon surface, as revealed by epifluorescent imaging (Figure 2(i) to (k)).

In CS-PRP treated shoulders, PMN cells were recruited to the bony trough, the lateral tunnels, the SSP tendon and the endomysial space between SSP muscle fibers at day 1 (Figure 2), day 7 (Figure 3) and day 14. Tears were still evident at the insertion site, for both groups, with CS-PRP and without CS-PRP, at day 7 post-surgery (Figure 3(b) and (f)), but not by day 14, where granulation tissue had filled the space. The structure of the SSP tendons was altered in all cases at days 7 and 14, where the residual native-appearing tendon tissue was surrounded by highly cellular and vascularized granulation tissue (Figure 3). New bone was forming at the lateral aspect of the humerus by day 7 in both groups, without and with

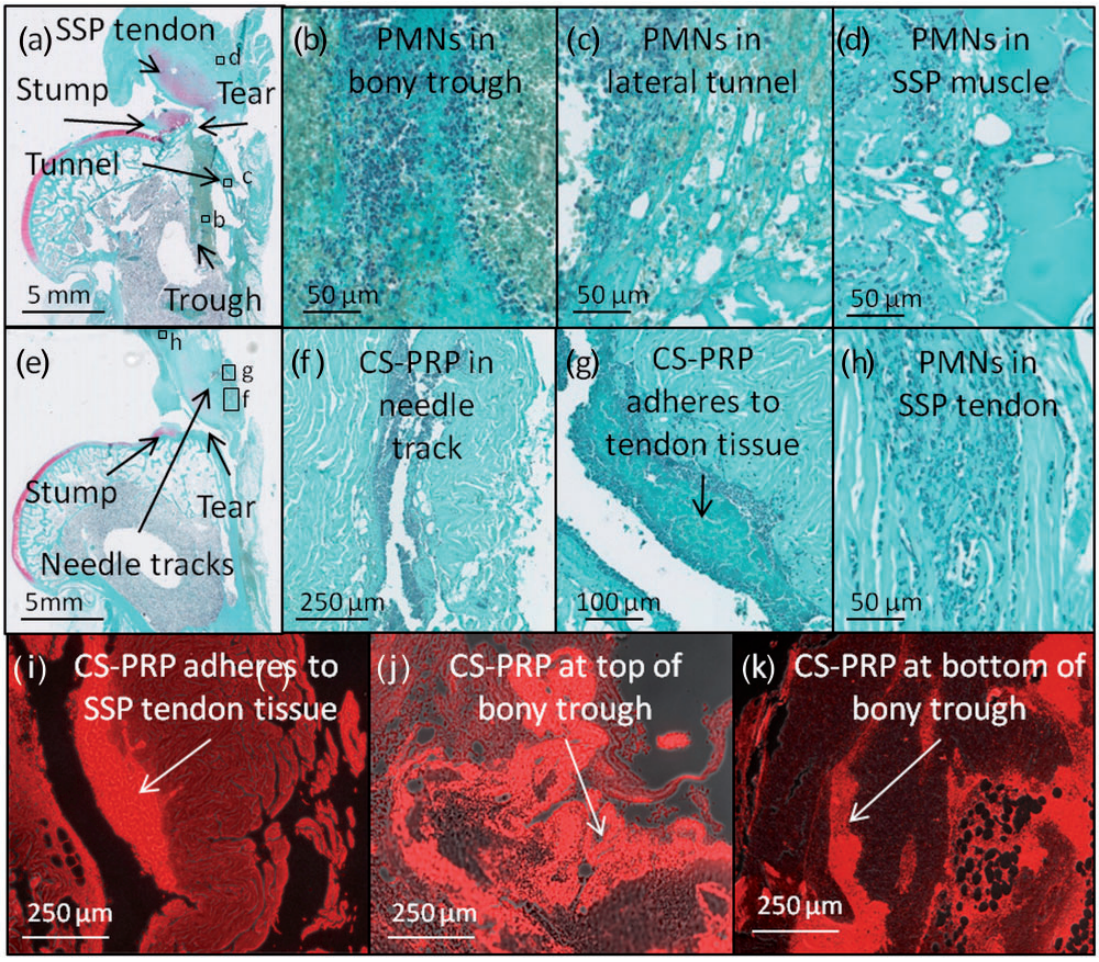

Figure 2. (a to h) Safranin O/Fast Green-stained paraffin sections of shoulder treated with transosseous suturing + CS-PRP after one day. Polymorphonuclear cells (PMNs) were recruited to the bony trough (b), to the lateral tunnels (c), to the endomyseal SSP muscle space (d) and to the SSP tendon (h). In some histological sections, needle tracks containing CS-PRP implant were visible within the SSP tendon (e & f). Note that stump of the tendon was not fully debrided in these samples (a and e). (i to k) A rhodamine-chitosan tracer was used to image chitosan with epifluorescence in bright red. At one day post-surgery, chitosan-PRP hybrid implant was found adhering to the SSP tendon surface (i) and in the bony trough (j & k).

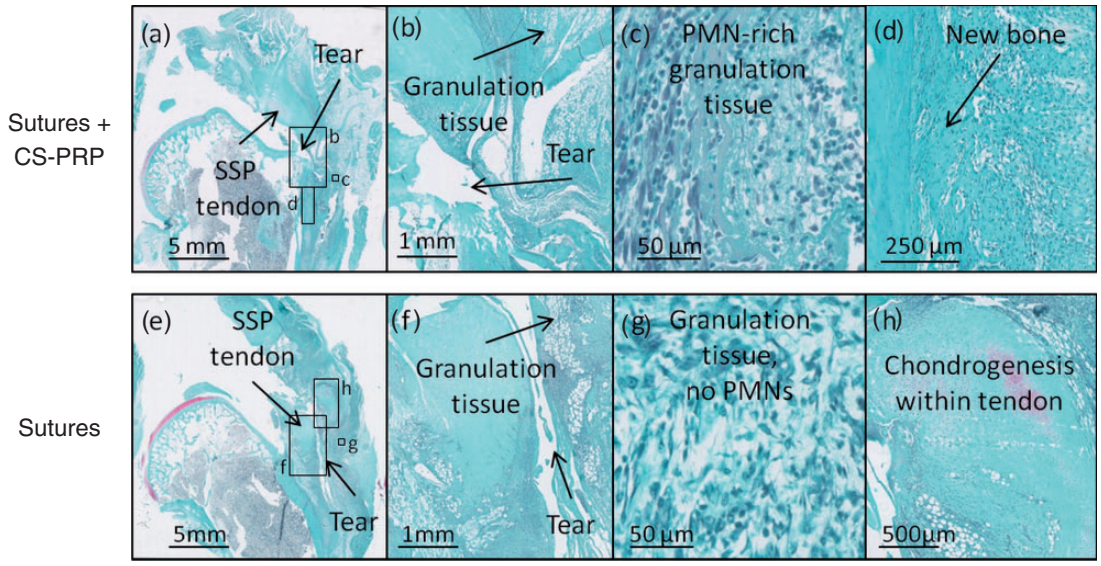

Figure 3. Safranin O/Fast Green-stained paraffin sections of shoulder treated with transosseous suturing + CS-PRP (a to d) or suturing only (e to h) after seven days. Residual structurally normal SSP tendon tissue was apparent and gaps were present at the tear site in all samples (a, b, e and f). Polymorphonuclear (PMN) cells were abundant in the granulation tissue of the CS-PRP treated shoulder only (c vs. g). New bone was forming at the lateral aspect of the cortical bone in both groups (example shown in d). Chondrogenesis was observed in the SSP tendon of the control sutured shoulder only (h). Outlines in (a) and (e) show where higher magnification images were acquired.

CS-PRP (See example in Figure 3(d)). Chondrogenesis was visible within the SSP tendon body at day 7, far from the insertion site, in the control-sutured shoulder only (Figure 3(h)), but not in the case of CS-PRP treatment. It is important to note that these early time point results were extrapolated from a low number of rabbits, and that only the two-month results described below are significant.

CS-PRP implants inhibited heterotopic ossification of SSP tendon tissue at two months

By two months post-surgery, significant remodeling of the SSP tendon structure had occurred in all shoulders, regardless of treatment (Figure 4(e) to (l)). SSP tendons were highly cellular and vascular compared to native intact tissues (Figure 4). Heterotopic bone formation was observed in five out of nine SSP tendons of control sutured shoulders and less frequently (in two out of nine cases) in the case of CS-PRP treatment ($p = 0.007$ comparing suturing only to suturing+CS-PRP; Figure 4(k) to (m)). In six out of nine shoulders treated with CS-PRP, PMNs were no longer visible at two months. However, in the remaining three shoulders, neutrophil-rich granulation tissue and areas of apoptotic or necrotic tissue was still apparent ($p < 0.0001$ comparing suturing+CS-PRP to suturing only; Figure 4(g), (h) and (m)). In contrast, there were no PMNs in any of the nine control sutured shoulders.

CS-PRP implants significantly improved attachment of SSP tendon at two months

The macroscopic attachment score (ranging from 0 for intact/native to 3 for detached) was better for shoulders treated with suturing + CS-PRP (average score of 1) compared to shoulders treated with suturing only (average score of 2). CS-PRP-treated shoulders also showed better microscopic SSP tendon attachment at the greater tuberosity ($p = 0.0333$ compared to suturing only) at two months (Figure 5(m)). In the best cases (Figure 5(f) and (j)), the enthesis had reformed with a partially calcified interface (in 14 out of 26 histological sections in the CS-PRP-treated shoulders and in seven out of 26 histological sections in the suturing only group). Polarized light microscopy (PLM) showed that collagen fibers were aligned parallel to the long axis of the SSP tendon in those cases, similar to the native intact enthesis (Figure 6(a), (c) and (e)). In the worst cases (Figure 5(h) and (l)), there were gaps between the humeral head and the repair tissue (in one out of 26 histological sections in the CS-PRP treated shoulders and in two out of 26 histological sections in the suturing only group).

CS-PRP implants induced bone remodelling at the greater tuberosity at two months

Micro-CT images showed that incomplete cortical bone repair at the lateral aspect of the humerus

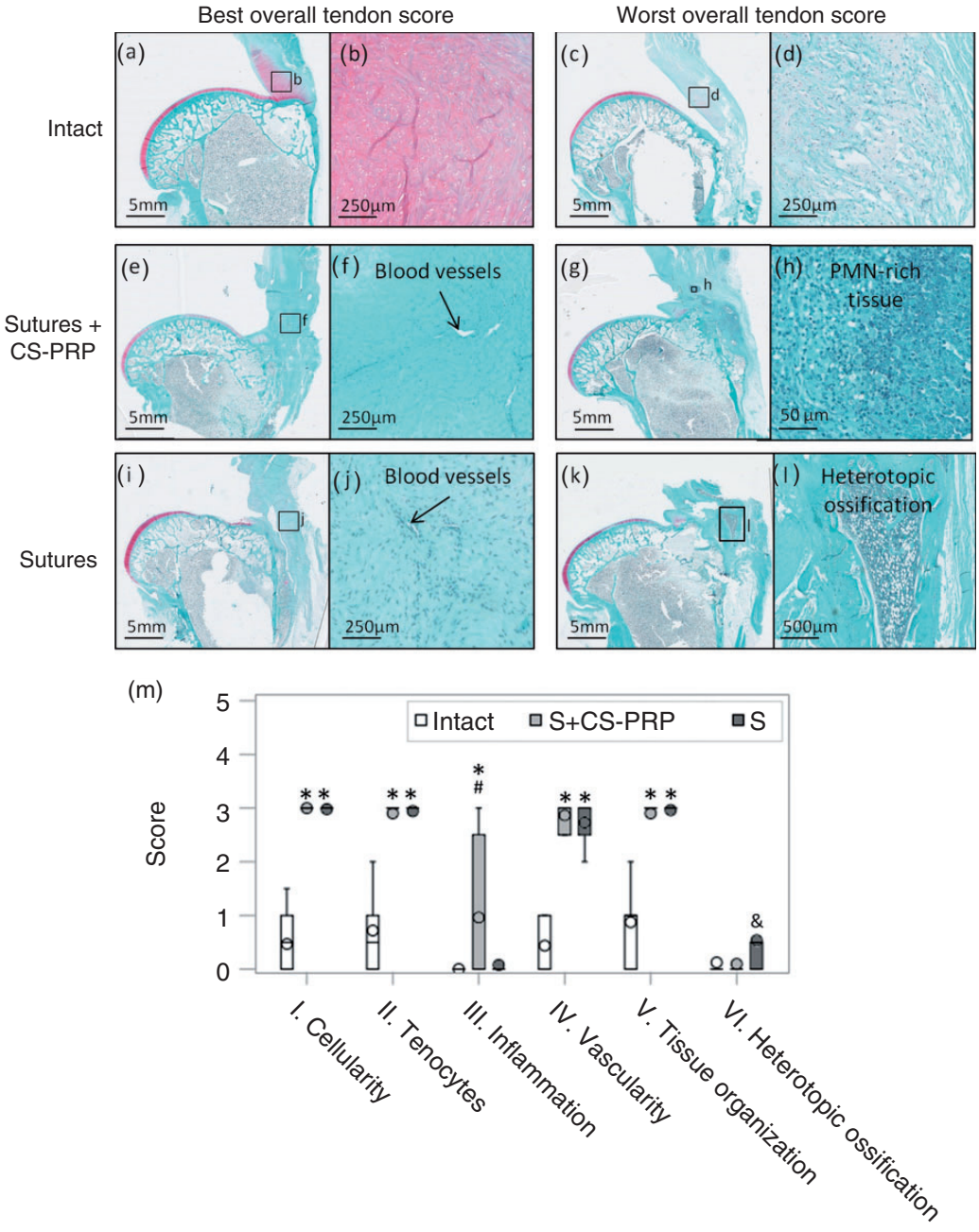

Figure 4. Safranin O/Fast Green-stained paraffin sections of intact shoulders (a to d), and test shoulders treated with transosseous suturing + CS-PRP (e to h) or suturing only (i to l) after two months, showing best and worst overall tendon scores for all groups. SSP tendon structure was altered in all surgically treated shoulders with several tendons displaying a highly cellular and vascular phenotype (e, f, i and j). Inflammatory PMN-rich tissue was present in three out nine shoulders treated with transosseous suturing + CS-PRP at two months (g & h). Heterotopic ossification within the SSP tendon was observed in five out of nine shoulders treated with transosseous suturing (k & l). Data in m are presented as mean (circle), median (line); Box: 25th and 75th percentile; Whisker: Box to the most extreme point within 1.5 interquartile range. *$p < 0.05$ compared to intact. #$p < 0.05$ compared to sutures group. & $p < 0.05$ compared to sutures + CS-PRP group.

(Figure 7(c) and (d)) and lateral outgrowth of bone (Figure 7(e) and (f)) were present in all shoulders, regardless of treatment. Incomplete repair of the bony troughs was observed bilaterally in five out of eight rabbits (Figure 7(g) and (h)), demonstrating variability in inherent capacity for bone repair between animals. In half the treated shoulders (four out of eight), bone remodeling was highly stimulated by CS-PRP treatment (Figure 7, compare panel c to d), which led to increases in bone surface (Figure 7(j)) and

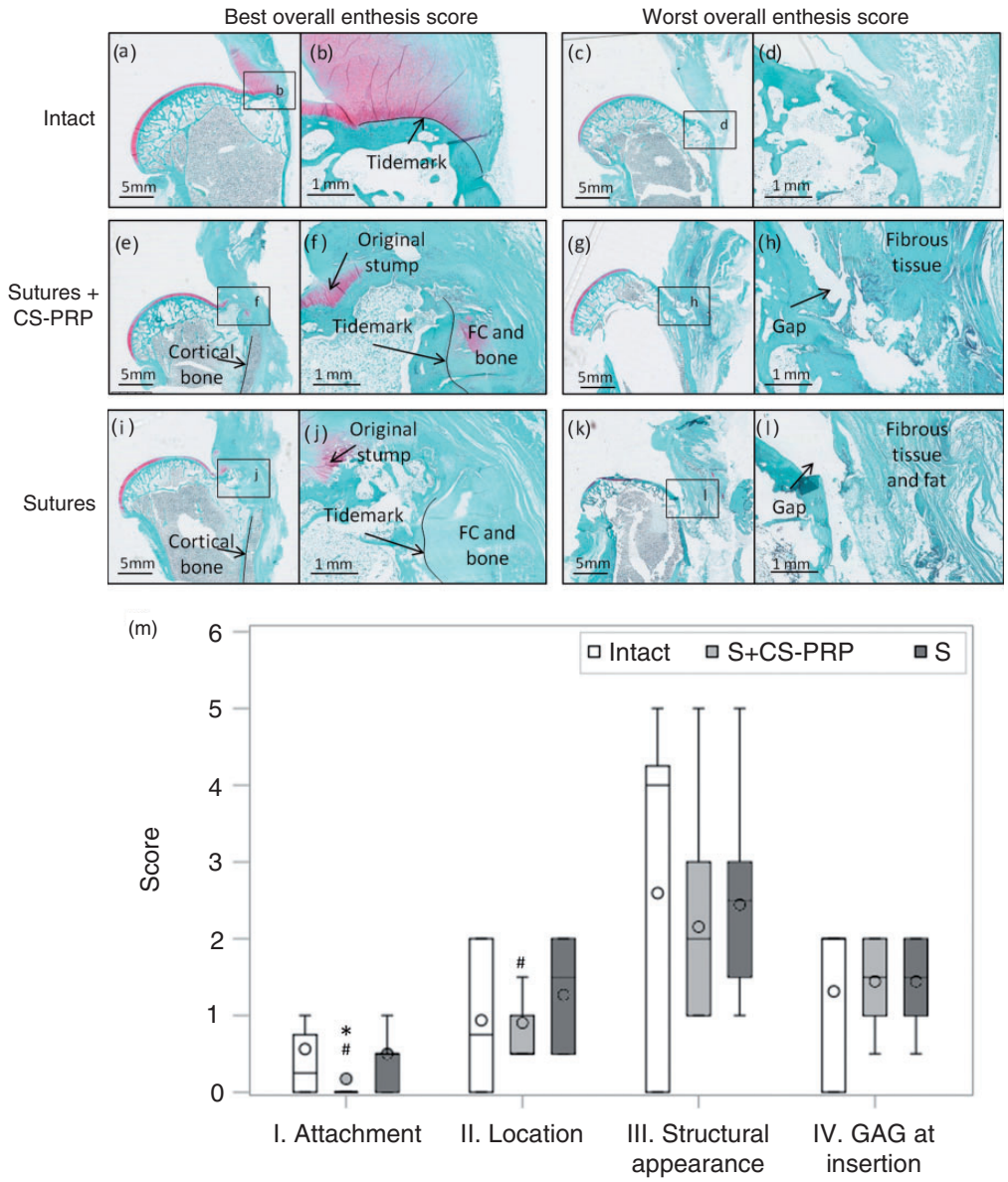

Figure 5. Safranin O/Fast Green-stained paraffin sections of intact shoulders (a to d), and test shoulders treated with transosseous suturing + CS-PRP (e to h) or suturing only (i to l) after two months, showing best and worst overall enthesis scores for all groups. The original tendon stump was often observed in surgically treated shoulders (e, f, i & j). In the best repair cases, fibrocartilage formation and partial restoration of the tidemark were observed at the enthesis (f & j). In the worst repair cases, gaps were present at the tendon-bone interface (h & l), although treatment with transosseous suturing + CS-PRP decreased such instances (m). Data in m are presented as mean (circle), median (line); Box: 25th and 75th percentile; Whisker: Box to the most extreme point within 1.5 interquartile range. *$p < 0.05$ compared to intact. #$p < 0.05$ compared to sutures group.

connectivity (Figure 7(k)). In addition, connectivity density and Euler number (a parameter that assesses bone connectivity) were also significantly increased by CS-PRP treatment, while there was no significant difference between the two groups for the other 3D bone morphometric parameters assessed (bone volume, trabecular thickness, trabecular separation, trabecular number, trabecular pattern factor, structural model index, fractal dimension and degree of anisotropy).

CS-PRP treatment was safe

Clinical and macroscopic observations showed that the CS-PRP formulation did not induce any adverse event in any of the rabbits. No infection, contracture, mobility disability, or excessive inflammatory reaction was observed. Body weights were stable throughout the study, and the surgical sites healed well with no sign of significant effusion. Some humeral head and glenoid

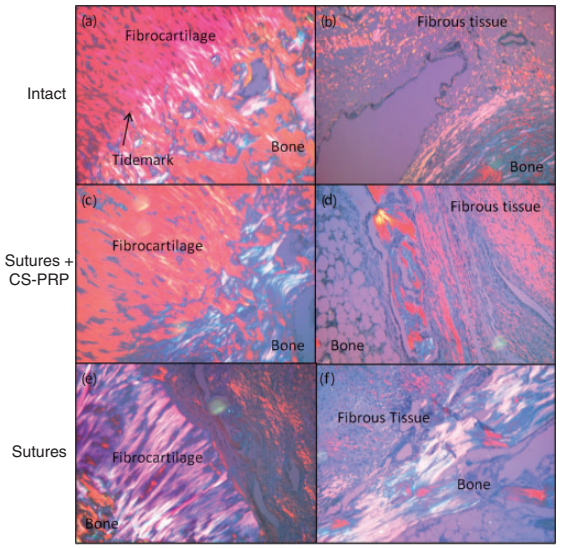

Figure 6. Polarized light microscopy images of SSP entheses. In the best cases, wave-like structures and alignment of the collagen fibres parallel to the long axis of the SSP tendon were visible (a, c & e). In the worst cases, very little collagen alignment was apparent in the fibrous tissue adjacent to the bone (b, d & f).

articular surfaces showed mild degenerative changes, such as GAG depletion (Figure 8(f), (h), (j), and (l)), hypocellularity and fissures (Figure 8(f) and (j)), hypercellularity (Figure 8(h)) and thinning (Figure 8(l)), although average histological scores were not significantly different than those of intact tissues (Figure 8 (m)). Surgical detachment and reattachment of the SSP tendon induced mild fatty infiltration of the SSP muscles compared to intact tissues (Figure 9). Finally, leukocyte percentage differential within the synovial fluid was similar for both groups, with and without CS-PRP treatment at two months.

Discussion

The aim of the current study was to histologically assess whether CS-PRP implants are capable of improving rotator cuff surgical repair. A transosseous repair model in the rabbit was chosen (Figure 1) since it has been well described in the literature.[23–29] Our data showed that CS-PRP implants were delivered effectively and did not induce degeneration of adjacent tissues compared to controls. In addition, CS-PRP implants induced PMN recruitment at early time points post-surgery, supporting our first hypothesis. In contrast to the second hypothesis, implant degradation and associated inflammatory reactions were still ongoing in three out of nine treated shoulders at two months. Results also partly supported our third hypothesis that CS-PRP would improve rotator cuff repair, since treatment improved SSP tendon attachment through increased bone remodeling. Other parameters assessed showed minimal improvement with CS-PRP treatment at this two-month post-repair time point.

One of our objectives was to determine implant distribution and assess implant degradation over time. At one day post-surgery, CS-PRP implants were resident inside the bony trough and lateral tunnels and also adhered to tendon surfaces (Figure 2), the latter probably due to the mucoadhesive properties of chitosan.[35] Similarly to CS-GP/blood implants, CS-PRP implants stimulated the innate immune response and induced recruitment of PMN cells (Figures 2 and 3), which contributed to implant degradation. It is well known that chitosans with higher degrees of deacetylation (DDA) and molar mass (M_n) will have lower degradation rates, but the site of implantation will also have a significant impact on implant degradation rate. We have previously shown that CS-PRP implants containing chitosan of similar DDA and M_n as that used in the current study were degraded after three weeks in sheep meniscus tears,[22] between three and eight weeks in rabbit cartilage lesions,[20] but that they persisted for at least six weeks in a rabbit subcutaneous implantation model.[19] Unexpectedly, small areas of neutrophil-rich granulation tissue surrounding apoptotic/necrotic tissues were visible in three out of nine CS-PRP treated shoulders at two months (Figure 4). This suggests that implant degradation was not complete in these animals, as residual apoptotic/necrotic granulation tissues were previously shown to correlate with resident chitosan oligomer particles in a rabbit cartilage repair model.[36] Alternatively, it is also possible that PMNs could persist for some time after complete chitosan degradation. A leukocyte-containing PRP was used to prepare the implants in the current study, which would be expected to have an impact on the cytokine profile that is released upon activation.[37,38] Previous *in vitro* studies have suggested that matrix metalloproteinases (MMP) and cytokines released from leukocyte-rich PRP could have deleterious effects on tendon healing.[39] However, MMPs are believed to be essential for tissue remodeling during rotator cuff tear repair *in vivo* and clinical data regarding using leukocyte-rich versus leukocyte-poor PRP for rotator cuff repair are still inconclusive.

The suppression of SSP tendon heterotopic ossification (HO) by CS-PRP treatment was an unexpected finding in this study (Figure 4). HO is an abnormal formation of mature, lamellar bone in soft tissues where bone normally does not exist.[40]HO is a well-known complication following surgical procedures or traumatic injuries.[41,42] Osteoinductive factors are released as a consequence of soft tissue trauma, thus potentially inducing formation of heterotopic bone.[43–45] The pathogenesis is unclear, but it may involve inappropriate differentiation of pluripotent mesenchymal stem cells (MSCs) into bone

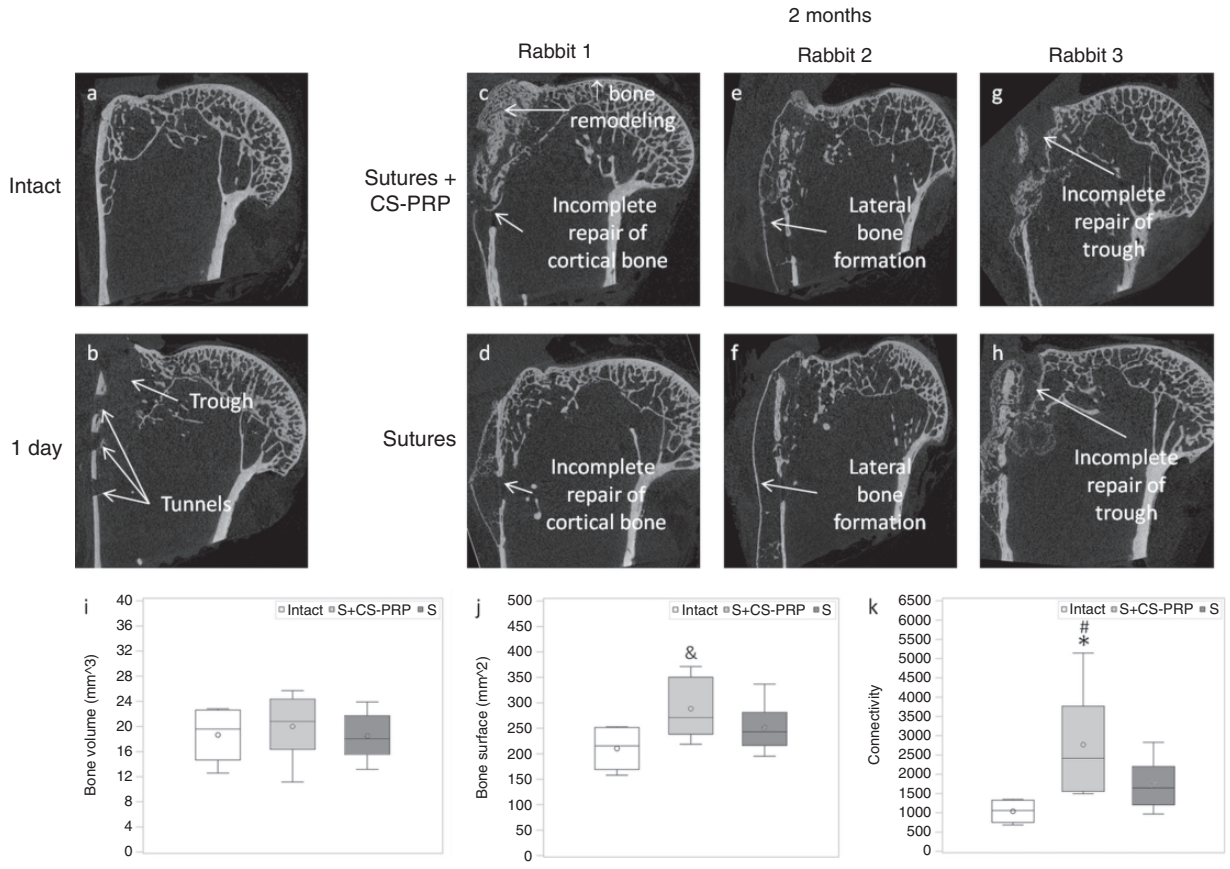

Figure 7. Micro-CT of intact (a) and surgically treated shoulder at one day (b), and test shoulders treated with transosseous suturing + CS-PRP (c to g) or suturing only (d to h) after two months. Incomplete repair of cortical bone at the lateral aspect of the humerus (c & d) and lateral bone formation (e & f) were present in all shoulders, regardless of treatment. Incomplete repair of the bone troughs was observed bilaterally in five rabbits (g & h). In half the treated shoulders, bone remodeling was highly stimulated by chitosan-PRP treatment (compare panel c to d), which led to increases in bone surface (j) and connectivity (k). Data in i, j & k are presented as mean (circle), median (line); Box: 25th and 75th percentile; Whisker: Box to the most extreme point within 1.5 interquartile range. *$p < 0.05$ compared to intact. #$p < 0.05$ compared to sutures group. &$p < 0.1$ compared to intact.

forming cells under growth factor influence.[46] HO occurs through endochondral ossification,[40] the first step of which is differentiation of MSCs into chondrocytes, an event we observed here in the control sutured shoulder at seven days (Figure 3), but not in the shoulder treated with CS-PRP. Interestingly, CS-GP/blood implants were also previously shown to modulate the timing and spatial development of chondrogenesis and endochondral ossification in a rabbit cartilage repair model.[47]

The bone surrounding the bony trough is a probable source of repair cells in this model, as are bursa or synovial-derived cells.[23] The tendon stump appeared to contribute little to healing, and was integrated within the new repair tissue at two months in most cases (Figure 5). Improving tendon-bone healing is a common clinical challenge in rotator cuff repair. Development of bone-tendon junction occurs through chondrogenesis and tenogenesis, followed by mineralization,[48–52] while tendon-bone repair appears to depend upon bone ingrowth into fibrovascular interface tissue. Surgical reattachment of rotator cuff tendon with current repair techniques leads to a more abrupt interface and a disorganized scar tissue that is mechanically inferior to the native interface,[53,54] and augmentation techniques still need to be developed to overcome this limitation. As reported previously,[23] enthesis regeneration was not achieved in the transosseous repair model used here; however, partial restoration of the calcified interface was more common with CS-PRP treatment (Figures 5 and 6). Growth factors synthesized and secreted by cells involved in tissue repair, such as platelets, inflammatory cells, fibroblasts, epithelial cells, and vascular endothelial cells,[55] all regulate tendon-bone repair, and it is likely that treatment with CS-PRP modulates such signals. It has previously

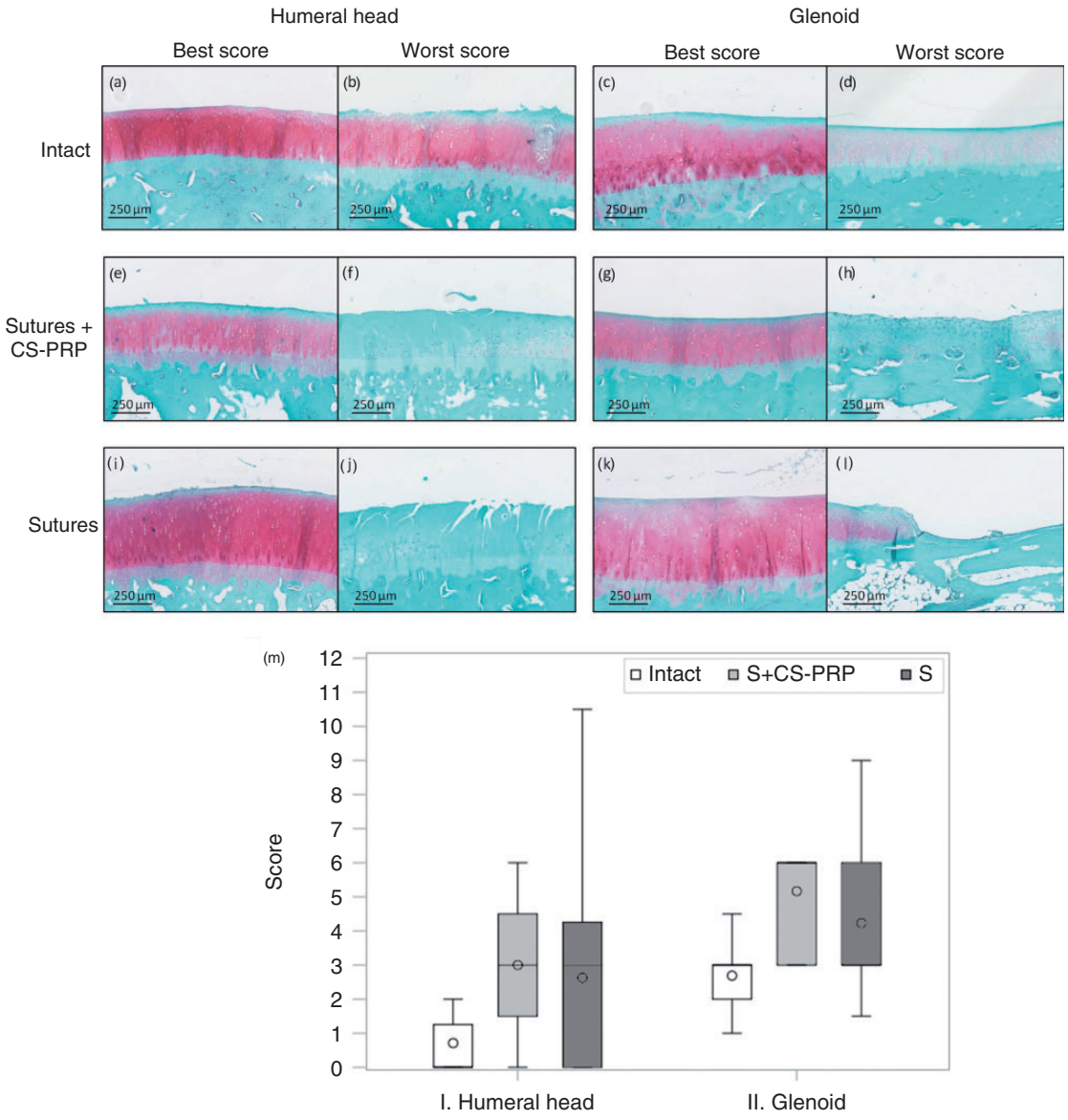

Figure 8. Safranin O/Fast Green-stained paraffin sections of intact shoulders (a to d), and test shoulders treated with transosseous suturing + CS-PRP (e to h) or suturing only (i to l) after two months, showing best and worst OOCHAS (OARSI Osteoarthritis Cartilage Histopathology Assessment System) scores for humeral head and glenoid articular surfaces (a to l). Some structural abnormalities such as GAG depletion, fissures, cell changes and thinning of the articular cartilage were occasionally observed in both humeral head (b, f & j) and glenoid (d, h & l) surfaces, although average histological scores were not significantly different from intact (m). Data in m are presented as mean (circle), median (line); Box: 25th and 75th percentile; Whisker: Box to the most extreme point within 1.5 interquartile range.

been shown by us and others that chitosan can increase release of platelet-derived growth factors when placed in contact with PRP,[19,56] and this may be one mechanism by which the implants modulate the healing response. Gap formation is thought to be associated with impaired rotator cuff healing,[57] preventing enthesis reformation.[28] CS-PRP treatment promoted attachment of the SSP tendon, possibly through an increase in bone remodeling at the greater tuberosity (Figure 7). Previous cartilage repair studies in the rabbit also showed that both CS-GP/blood implants and CS-PRP implants promote bone remodeling and tissue integration.[14,15,17,20] The bony trough was incompletely healed in some rabbits, consistent with previously published data showing that complete recovery of the bony trough only occurs after 12 weeks post-surgery in this model.[24]

No treatment-specific adverse events occurred during the study, which suggests high safety. Surgical detachment and immediate reattachment of the SSP

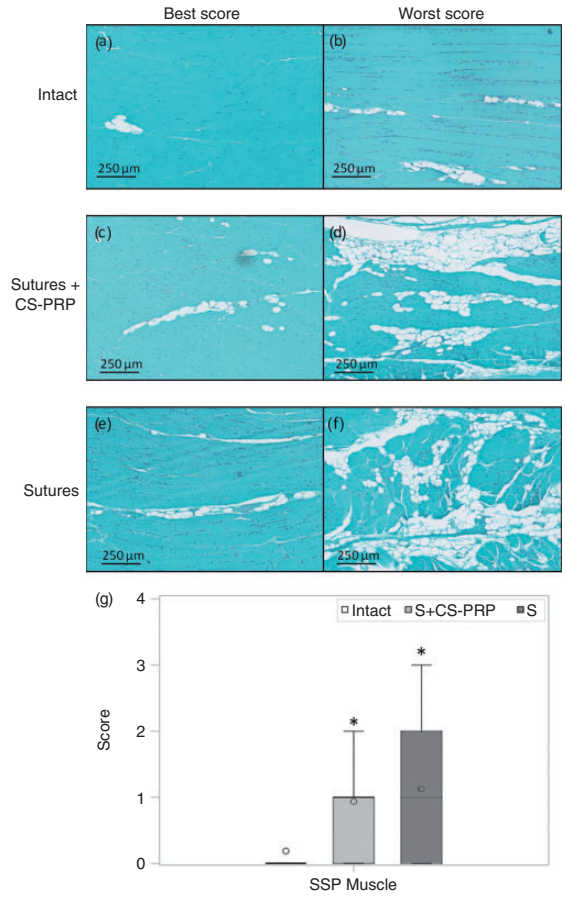

Figure 9. Safranin O/Fast Green-stained paraffin sections of SSP muscles from intact shoulders (a & b), and test shoulders treated with transosseous suturing + CS-PRP (c & d) or suturing only (e & f) after two months, showing best and worst scores for fatty infiltration. Surgical treatment induced fatty infiltration of SSP muscle after two months (g). Data in g are presented as mean (circle), median (line); Box: 25th and 75th percentile; Whisker: Box to the most extreme point within 1.5 interquartile range. *$p < 0.05$ compared to intact.

tendon was sufficient to cause fatty infiltration of the SSP muscle but did not induce degeneration of the humeral head and glenoid articular surfaces (Figures 8 and 9), while treatment with CS-PRP did not alter the cell distribution within the synovial fluid of the shoulder. Another surprising finding of this study was the significant variability of the histological appearance of the SSP tendons and entheses within the intact group (Figures 4 to 6). The sections with the best overall scores were structurally normal, but several tendons and entheses from intact un-operated animals displayed features that suggest that some spontaneous degeneration can occur in the rabbit model. A larger sample size would have allowed us to identify outliers. Although the tendons appeared macroscopically normal in the surgically treated animals intra-operatively, spontaneous degeneration would be expected to impact healing responses if present.

This study had several limitations. No animal model fully reproduces human injury condition. The shoulder joints are weight-bearing in rabbits and acute tears do not represent human chronic degenerative tears. However, we chose this model since the rotator cuff in rabbits heals in a fashion that is similar to that of humans.[58] Additionally, the rabbit model allowed us to collect enough blood to extract the required PRP volume to solubilize the freeze-dried chitosan. Another limitation is that the transosseous repair technique used here differs from suture anchors which are more commonly used in humans. However, use of suture anchors would be difficult due to the small size of the glenohumeral joint in rabbits. The inability to limit weight bearing and activity post-operatively may contribute to sutures pulling out of the rabbit tendon. We did not include a suturing+PRP group here as an additional control since use of PRP is not currently standard of care, as recent studies are inconclusive as to whether PRP alone improves rotator cuff repair. However, it will be imperative to conduct a comparative study with a control group receiving treatment with suturing+PRP alone in order to distinguish between the effects arising from chitosan-PRP and from PRP alone. Moreover, the small sample size at early time points is a significant limitation of the study and does not allow us to elaborate on the mechanisms involved in the repair process and draw firm conclusions. Finally, although a histological improvement in SSP tendon attachment would be expected to translate into superior attachment strength, no biomechanical testing was performed.

Conclusion

Rotator cuff repair remains a pressing clinical challenge. Despite our study's limitations, our preliminary study showed that CS-PRP implants were retained at the site of injection and did not induce deleterious effects in the joint. In addition, using CS-PRP implants in conjunction with transosseous suturing improved attachment of the SSP tendon to the humeral head compared to suturing alone. This study provides the first evidence that CS-PRP implants are safe and possibly effective in improving rotator cuff tear repair in a small animal model, and that this could potentially be translated to a larger animal model and then to a clinical setting. Future work should involve a larger number of animals, multiple time points with a longer duration of follow-up, additional control groups, as well as histomorphometric, immunohistochemical, and biomechanical testing to fully assess the implant's efficacy.

Acknowledgements

We acknowledge the technical contributions of Jun Sun and Geneviève Picard.

Declaration of Conflicting Interests

The author(s) declared the following potential conflicts of interest with respect to the research, authorship, and/or publication of this article: AC and MDB hold shares, MDB is a director and MS and SR are clinical advisors of Ortho Regenerative Technologies Inc.

Funding

The author(s) disclosed receipt of the following financial support for the research, authorship, and/ or publication of this article: Funding sources for this work include the Canadian Institutes of Health Research, Canada Foundation for Innovation, Groupe de Recherche en Sciences et Technologies Biomédicales, Natural Sciences and Engineering Research Council of Canada and Ortho Regenerative Technologies Inc.

ORCID iD

Michael D Buschmann http://orcid.org/0000-0001-7555-8189

References

1. Lehman C, Cuomo F, Kummer FJ, et al. The incidence of full thickness rotator cuff tears in a large cadaveric population. *Bull Hosp Jt Dis* 1995; 54: 30–31.
2. Barber FA, Hrnack SA, Snyder SJ, et al. Rotator cuff repair healing influenced by platelet-rich plasma construct augmentation. *Arthroscopy* 2011; 27: 1029–1035.
3. Galatz LM, Ball CM, Teefey SA, et al. The outcome and repair integrity of completely arthroscopically repaired large and massive rotator cuff tears. *J Bone Joint Surg-Am* 2004; 86A: 219–224.
4. Gulotta LV and Rodeo SA. Growth factors for rotator cuff repair. *Clin Sports Med* 2009; 28: 13–23.
5. Chung SW, Kim SH and Oh JH. Animal experiments using rotator cuff. *Clin Should Elb* 2014; 17: 84–90.
6. Deprés-Tremblay G, Chevrier A, Snow M, et al. Rotator cuff repair: a review of surgical techniques, animal models, and new technologies under development. *J Should Elb Surg*. 2016; 25: 2078–2085.
7. Dohan Ehrenfest DM, Rasmusson L and Albrektsson T. Classification of platelet concentrates: from pure platelet-rich plasma (P-PRP) to leucocyte- and platelet-rich fibrin (L-PRF). *Trends Biotechnol* 2009; 27: 158–167.
8. Vavken P, Sadoghi P, Palmer M, et al. Platelet-rich plasma reduces retear rates after arthroscopic repair of small- and medium-sized rotator cuff tears but is not cost-effective. *Am J Sports Med* 2015; 43: 3071–3076. DOI: 10.1177/0363546515572777.
9. Li X, Xu C-P, Hou Y-L, et al. Are platelet concentrates an ideal biomaterial for arthroscopic rotator cuff repair? A meta-analysis of randomized controlled trials. *Arthroscopy* 2014; 30: 1483–1490.
10. Zhao J-G, Zhao L, Jiang Y-X, et al. Platelet-rich plasma in arthroscopic rotator cuff repair: a meta-analysis of randomized controlled trials. *Arthroscopy* 2015; 31: 125–135.
11. Warth RJ, Dornan GJ, James EW, et al. Clinical and structural outcomes after arthroscopic repair of full-thickness rotator cuff tears with and without platelet-rich product supplementation: a meta-analysis and meta-regression. *Arthroscopy* 2015; 31: 306–320.
12. Muzzarelli RAA. Chitins and chitosans for the repair of wounded skin, nerve, cartilage and bone. *Carb Polym* 2009; 76: 167–182.
13. Cheung RCF, Ng TB, Wong JH, et al. Chitosan: an update on potential biomedical and pharmaceutical applications. *Marine Drugs* 2015; 13: 5156–5186.
14. Chevrier A, Hoemann CD, Sun J, et al. Chitosan-glycerol phosphate/blood implants increase cell recruitment, transient vascularization and subchondral bone remodeling in drilled cartilage defects. *Osteoarthr Cart* 2007; 15: 316–327.
15. Hoemann CD, Sun J, McKee MD, et al. Chitosan-glycerol phosphate/blood implants elicit hyaline cartilage repair integrated with porous subchondral bone in microdrilled rabbit defects. *Osteoarthr Cart* 2007; 15: 78–89.
16. Hoemann CD, Chen G, Marchand C, et al. Scaffold-guided subchondral bone repair implication of neutrophils and alternatively activated arginase-1+macrophages. *Am J Sports Med* 2010; 38: 1845–1856.
17. Chen G, Sun J, Lascau-Coman V, et al. Acute osteoclast activity following subchondral drilling is promoted by chitosan and associated with improved cartilage repair tissue integration. *Cartilage* 2011; 2: 173–185.
18. Chevrier A, Darras V, Picard G, et al. Injectable chitosan-platelet-rich plasma (PRP) implants to promote tissue regeneration: in vitro properties, in vivo residence, degradation, cell recruitment and vascularization. *J Tissue Eng Regen Med* 2018; 12: 217–228.
19. Deprés-Tremblay G, Chevrier A, Tran-Khanh N, et al. Chitosan inhibits platelet-mediated clot retraction, increases platelet-derived growth factor release, and increases residence time and bioactivity of platelet-rich plasma in vivo. *Biomed Mater* 2017; 13: 015005.
20. Dwivedi G, Chevrier A, Hoemann CD, et al. *Freeze dried chitosan/platelet-rich-plasma implants improve marrow stimulated cartilage repair in rabbit chronic defect model*. San Diego, CA: Transactions Orthopaedic Research Society, 2017.
21. Ghazi Zadeh L, Chevrier A, Hurtig MB, et al. *Freeze-dried chitosan-PRP injectable surgical implants for meniscus repair: results from pilot ovine studies*. San Diego, CA: Transactions Orthopaedic Research Society, 2017.
22. Chevrier A, Deprés-Tremblay G, Hurtig MB, et al. *Chitosan-platelet-rich plasma implants can be injected into meniscus defects to improve repair*. Orlando, FL: Transactions Orthopaedic Research Society, 2016.
23. Uhthoff HK, Sano H, Trudel G, et al. Early reactions after reimplantation of the tendon of supraspinatus into

bone. A study in rabbits. *J Bone Joint Surg Br* 2000; 82: 1072–1076..
24. Uhthoff HK, Seki M, Backman DS, et al. Tensile strength of the supraspinatus after reimplantation into a bony trough: an experimental study in rabbits. *J Shoulder Elbow Surg* 2002; 11: 504–509. 2002/10/16.
25. Uhthoff HK, Matsumoto F, Trudel G, et al. Early reattachment does not reverse atrophy and fat accumulation of the supraspinatus–an experimental study in rabbits. *J Orthop Res* 2003; 21: 386–392.
26. Koike Y, Trudel G and Uhthoff HK. Formation of a new enthesis after attachment of the supraspinatus tendon: a quantitative histologic study in rabbits. *J Orthop Res* 2005; 23: 1433–1440.
27. Koike Y, Trudel G, Curran D, et al. Delay of supraspinatus repair by up to 12 weeks does not impair enthesis formation: a quantitative histologic study in rabbits. *J Orthop Res* 2006; 24: 202–210.
28. Trudel G, Ramachandran N, Ryan SE, et al. Improved strength of early versus late supraspinatus tendon repair: a study in the rabbit. *J Should Elb Surg* 2012; 21: 828–834..
29. Trudel G, Ryan SE, Rakhra K, et al. Muscle tissue atrophy, extramuscular and intramuscular fat accumulation, and fat gradient after delayed repair of the supraspinatus tendon: a comparative study in the rabbit. *J Orthop Res* 2012; 30: 781–786.
30. Ma O, Lavertu M, Sun J, et al. Precise derivatization of structurally distinct chitosans with rhodamine B isothiocyanate. *Carb Polym* 2008; 72: 616–624.
31. Gonshor A. Technique for producing platelet-rich plasma and platelet concentrate: background and process. *Int J Period Rest Dent* 2002; 22: 547–557.
32. Watkins JP, Auer JA, Gay S, et al. Healing of surgically created defects in the equine superficial digital flexor tendon: collagen-type transformation and tissue morphologic reorganization. *Am J Vet Res* 1985; 46: 2091–2096.
33. Ide J, Kikukawa K, Hirose J, et al. The effect of a local application of fibroblast growth factor-2 on tendon-to-bone remodeling in rats with acute injury and repair of the supraspinatus tendon. *J Should Elb Surg* 2009; 18: 391–398.
34. Pritzker KP, Gay S, Jimenez SA, et al. Osteoarthritis cartilage histopathology: grading and staging. *Osteoarthr Cart* 2006; 14: 13–29.
35. Henriksen I, Green KL, Smart JD, et al. Bioadhesion of hydrated chitosans: An in vitro and in vivo study. *Int J Pharm* 1996; 145: 231–240.
36. Lafantaisie-Favreau CH, Guzman-Morales J, Sun J, et al. Subchondral pre-solidified chitosan/blood implants elicit reproducible early osteochondral wound-repair responses including neutrophil and stromal cell chemotaxis, bone resorption and repair, enhanced repair tissue integration and delayed matrix deposition. *BMC Musculoskel Dis* 2013; 14: 1–16.
37. Dragoo JL, Braun HJ, Durham JL, et al. Comparison of the acute inflammatory response of two commercial platelet-rich plasma systems in healthy rabbit tendons. *Am J Sports Med* 2012; 40: 1274–1281.
38. McCarrel TM, Minas T and Fortier LA. Optimization of leukocyte concentration in platelet-rich plasma for the treatment of tendinopathy. *J Bone Joint Surg-Am* 2012; 94: 141–148.
39. Fabis J, Kordek P, Bogucki A, et al. Function of the rabbit supraspinatus muscle after detachment of its tendon from the greater tubercle – Observations up to 6 months. *Acta Orthop Scand* 1998; 69: 570–574.
40. Zhang J, Zhao Y, Hou X, et al. The inhibition effects of insulin on BMP2-induced muscle heterotopic ossification. *Biomaterials* 2014; 35: 9322–9331.
41. Barfield WR, Holmes RE and Hartsock LA. Heterotopic ossification in trauma. *Orthop Clin North Am* 2017; 48: 35–46. 2016/11/26. DOI: 10.1016/j.ocl.2016.08.009.
42. Balboni TA, Gobezie R and Mamon HJ. Heterotopic ossification: pathophysiology, clinical features, and the role of radiotherapy for prophylaxis. *Int J Rad Onc Biol Phys* 2006; 65: 1289–1299.
43. Sneath RJ, Bindi FD, Davies J, et al. The effect of pulsed irrigation on the incidence of heterotopic ossification after total hip arthroplasty. *J Arthroplasty* 2001; 16: 547–551.
44. Nilsson OS and Persson PE. Heterotopic bone formation after joint replacement. *Curr Opin Rheumatol* 1999; 11: 127–131.
45. Chalmers J, Gray DH and Rush J. Observations on the induction of bone in soft tissues. *J Bone Joint Surg Br* 1975; 57: 36–45.
46. Lewallen DG. Heterotopic ossification following total hip arthroplasty. *Instr Course Lect* 1995; 44: 287–292.
47. Chevrier A, Hoemann CD, Sun J, et al. Temporal and spatial modulation of chondrogenic foci in subchondral microdrill holes by chitosan-glycerol phosphate/blood implants. *Osteoarthr Cart* 2011; 19: 136–144.
48. Rees JD, Wilson AM and Wolman RL. Current concepts in the management of tendon disorders. *Rheumatology* 2006; 45: 508–521.
49. Lin TW, Cardenas L and Soslowsky LJ. Biomechanics of tendon injury and repair. *J Biomec* 2004; 37: 865–877.
50. Hamada Y, Katoh S, Hibino N, et al. Effects of monofilament nylon coated with basic fibroblast growth factor on endogenous intrasynovial flexor tendon healing. *J Hand Surg* 2006; 31: 530–540.
51. Lu HH and Thomopoulos S. Functional attachment of soft tissues to bone: development, healing, and tissue engineering. *Annu Rev Biomed Eng* 2013; 15: 201–226.
52. Thomopoulos S, Genin GM and Galatz LM. The development and morphogenesis of the tendon-to-bone insertion – what development can teach us about healing. *J Musculoskelet Neuronal Interact* 2010; 10: 35–45.
53. Thomopoulos S, Hattersley G, Rosen V, et al. The localized expression of extracellular matrix components in healing tendon insertion sites: an in situ hybridization study. *J Orthop Res* 2002; 20: 454–463.
54. Thomopoulos S, Williams GR and Soslowsky LJ. Tendon to bone healing: differences in biomechanical, structural, and compositional properties due to a range of activity levels. *J Biomech Eng* 2003; 125: 106–113.

55. Kobayashi M, Itoi E, Minagawa H, et al. Expression of growth factors in the early phase of supraspinatus tendon healing in rabbits. *J Should Elb Surg* 2006; 15: 371–377.
56. Hattori H and Ishihara M. Feasibility of improving platelet-rich plasma therapy by using chitosan with high platelet activation ability. *Exp Ther Med* 2017; 13: 1176–1180.
57. Omi R, Gingery A, Steinmann SP, et al. Rotator cuff repair augmentation in a rat model that combines a multilayer xenograft tendon scaffold with bone marrow stromal cells. *J Should Elb Surg* 2016; 25: 469–477.
58. Gupta R and Lee TQ. Contributions of the different rabbit models to our understanding of rotator cuff pathology. *J Should Elb Surg* 2007; 16: 149S–157S.